International Journal of
Molecular Sciences

MDPI

Review

Effective Perturbations by Small-Molecule Modulators on Voltage-Dependent Hysteresis of Transmembrane Ionic Currents

Sheng-Nan Wu [1,2,3,*], Chao-Liang Wu [4], Hsin-Yen Cho [1] and Chi-Wu Chiang [5]

[1] Department of Physiology, National Cheng Kung University Medical College, Tainan 70101, Taiwan
[2] Institute of Basic Medical Sciences, National Cheng Kung University Medical College, Tainan 70101, Taiwan
[3] Department of Post-Baccalaureate Medicine, National Sun Yat-sen University, Kaohsiung 804201, Taiwan
[4] Department of Medical Research, Ditmanson Medical Foundation Chia-Yi Christian Hospital, Chiayi City 60002, Taiwan
[5] Institute of Molecular Medicine, College of Medicine, National Cheng Kung University, Tainan 70101, Taiwan
* Correspondence: snwu@mail.ncku.edu.tw; Tel.: +886-6-2353535 (ext. 5334); Fax: +886-6-2362780

Abstract: The non-linear voltage-dependent hysteresis ($Hys_{(V)}$) of voltage-gated ionic currents can be robustly activated by the isosceles-triangular ramp voltage (V_{ramp}) through digital-to-analog conversion. Perturbations on this $Hys_{(V)}$ behavior play a role in regulating membrane excitability in different excitable cells. A variety of small molecules may influence the strength of $Hys_{(V)}$ in different types of ionic currents elicited by long-lasting triangular V_{ramp}. Pirfenidone, an anti-fibrotic drug, decreased the magnitude of I_h's $Hys_{(V)}$ activated by triangular V_{ramp}, while dexmedetomidine, an agonist of α_2-adrenoceptors, effectively suppressed I_h as well as diminished the $Hys_{(V)}$ strength of I_h. Oxaliplatin, a platinum-based anti-neoplastic drug, was noted to enhance the I_h's $Hys_{(V)}$ strength, which is thought to be linked to the occurrence of neuropathic pain, while honokiol, a hydroxylated biphenyl compound, decreased I_h's $Hys_{(V)}$. Cell exposure to lutein, a xanthophyll carotenoid, resulted in a reduction of I_h's $Hys_{(V)}$ magnitude. Moreover, with cell exposure to UCL-2077, SM-102, isoplumbagin, or plumbagin, the $Hys_{(V)}$ strength of *erg*-mediated K^+ current activated by triangular V_{ramp} was effectively diminished, whereas the presence of either remdesivir or QO-58 respectively decreased or increased $Hys_{(V)}$ magnitude of M-type K^+ current. Zingerone, a methoxyphenol, was found to attenuate $Hys_{(V)}$ (with low- and high-threshold loops) of L-type Ca^{2+} current induced by long-lasting triangular V_{ramp}. The $Hys_{(V)}$ properties of persistent Na^+ current ($I_{Na(P)}$) evoked by triangular V_{ramp} were characterized by a figure-of-eight (i.e., ∞) configuration with two distinct loops (i.e., low- and high-threshold loops). The presence of either tefluthrin, a pyrethroid insecticide, or *t*-butyl hydroperoxide, an oxidant, enhanced the $Hys_{(V)}$ strength of $I_{Na(P)}$. However, further addition of dapagliflozin can reverse their augmenting effects in the $Hys_{(V)}$ magnitude of the current. Furthermore, the addition of esaxerenone, mirogabalin, or dapagliflozin was effective in inhibiting the strength of $I_{Na(P)}$. Taken together, the observed perturbations by these small-molecule modulators on $Hys_{(V)}$ strength in different types of ionic currents evoked during triangular V_{ramp} are expected to influence the functional activities (e.g., electrical behaviors) of different excitable cells in vitro or in vivo.

Keywords: voltage-dependent hysteresis; hyperpolarization-activated cation current; *erg*-mediated K^+ current; M-type K^+ current; L-type Ca^{2+} current; persistent Na^+ current; small-molecule modulators

Citation: Wu, S.-N.; Wu, C.-L.; Cho, H.-Y.; Chiang, C.-W. Effective Perturbations by Small-Molecule Modulators on Voltage-Dependent Hysteresis of Transmembrane Ionic Currents. *Int. J. Mol. Sci.* **2022**, *23*, 9453. https://doi.org/10.3390/ijms23169453

Academic Editor: Wolfgang Graier

Received: 3 August 2022
Accepted: 18 August 2022
Published: 21 August 2022

1. Introduction

Previous electrophysiological measurements with voltage-clamp maneuvers have used rectangular waveforms with varying durations of command voltages to evoke different types of voltage-gated ionic currents in attempts to evaluate the quasi-steady-state

relationship of current versus voltage in specified ionic currents. However, recent investigations have revealed that through efficient data acquisition with digital-to-analog conversion, the voltage-clamp protocol with different waveforms (e.g., triangular ramp voltage (V_{ramp})) can be specifically designed and exploited, and as whole-cell configuration was established, the voltage protocol can be thereafter applied to the tested cells. As a result, the non-linear relationship of current trace versus membrane potential (i.e., voltage-dependent hysteresis ($Hys_{(V)}$) can be activated. Such voltage dependence of different ionic currents can shift to either negative or positive potentials following activation, displaying a behavior analogous to that of ferromagnetic materials [1,2]. Of note, the $Hys_{(V)}$'s phenomenon residing in different types of transmembrane ionic currents has been viewed to be linked to conformational changes in the voltage sensor of the channel specified, and it has been also demonstrated to play an essential role in influencing the electrical behaviors of variable excitable cells [2].

In this review article, we intended to demonstrate that several intriguing small molecules interact with different types of transmembrane ionic currents to alter the behavior of $Hys_{(V)}$. The non-equilibrium $Hys_{(V)}$ properties residing in different types of ionic currents were mostly activated by the upright or inverted isosceles-triangular V_{ramp} through digital-to-analog conversion. The ionic currents involved include hyperpolarization-activated cation current (I_h), *erg*-mediated K^+ current ($I_{K(erg)}$), M-type K^+ current ($I_{K(M)}$), L-type Ca^{2+} current ($I_{Ca,L}$), and persistent Na^+ current ($I_{Na(P)}$) (Table 1). The $Hys_{(V)}$ occurrence induced during triangular V_{ramp} is thought to reflect that a mode shift during channel activation may exist since the voltage sensitivity of the gating charge movement relies on the previous state (conformation) of the channel involved [2]. Several small-molecule modulators have been found to regulate the $Hys_{(V)}$ strength occurring in different types of ionic currents (Table 1).

Table 1. Summary in the perturbations of the known small-molecule modulators on voltage-dependent hysteresis ($Hys_{(V)}$) behavior occurring in different types of ionic currents present in excitable cells (e.g., pituitary GH_3 lactotrophs).

Associated Ionic Currents	Small Molecules
hyperpolarization-activated cation current (I_h)	pirfenidone, oxaliplatin, lutein, dexmedetomidine, honokiol
erg-mediated K^+ current ($I_{K(erg)}$)	UCL-2077, SM-102, isoplumbagin, plumbagin
M-type K^+ current ($I_{K(M)}$)	remdesivir, QO-58
L-type Ca^{2+} current ($I_{Ca,L}$)	zingerone
persistent Na^+ current ($I_{Na(P)}$)	esaxerenone, tefluthrin, *t*-butyl hydroperoxide, mirogabalin, and dapagliflozin

2. $Hys_{(V)}$ Behavior Residing in Hyperpolarization-Activated Cation Current (I_h)

2.1. Pirfenidone (Esbriet®, 5-Methyl-1-Phenylpyridin-2[H-1]-One)

The magnitude of I_h (or funny current [I_f]) has been viewed to be a notable determinant of repetitive electrical activities inherently in heart cells and various excitable cells [3–9]. This type of ionic current is characterized by a mixed inward Na^+/K^+ current with a slowly activating property during long-lasting membrane hyperpolarization. Pirfenidone is thought to act by interfering with the production of transforming growth factor-β and tumor necrosis factor-α and it is a new anti-fibrotic drug for idiopathic pulmonary fibrosis [10]. Of note, a recent paper has convincingly demonstrated the ability of pirfenidone to produce a reduction in the $Hys_{(V)}$'s strength of I_h evoked by long-lasting inverted triangular V_{ramp} [11,12]. In other words, there was a substantial reduction in Δarea of I_h's $Hys_{(V)}$ loop encircled by the forward and backward limbs of the inverted double V_{ramp}. The experimental results thus suggest that cell exposure to pirfenidone can diminish such $Hys_{(V)}$ entailed in the voltage-dependent elicitation of I_h. The inhibitory effect of pirfenidone on I_h was also accompanied by substantial depression in the magnitude of

sag voltage elicited by hyperpolarizing current stimulus as observed under current-clamp potential recordings. However, neither the amplitude of $I_{K(M)}$ nor $I_{K(erg)}$ was altered by the presence of this compound. Therefore, these results highlight evidence that pirfenidone is capable of perturbing the magnitude, gating kinetics, and $Hys_{(V)}$ properties of I_h, thereby revealing a potential additional impact on the functional activities (e.g., discharge patterns) of different excitable cells.

2.2. Dexmedetomidine

Dexmedetomidine, a lipophilic imidazole derivative, is a potent and selective agonist of α_2-adrenergic receptors [13]. This drug has been disclosed to exert a variety of actions on the human brain such as sedation, anesthetic sparing effects, and analgesia [13,14]. A recent investigation has shown that dexmedetomidine could perturb on the non-equilibrium property of I_h in response to triangular V_{ramp} found in GH_3 cells [15]. The presence of this agent was found to diminish such $Hys_{(V)}$ linked to the voltage-dependent elicitation of I_h. However, further application of yohimbine, dexmedetomidine failed to attenuate dexmedetomidine-mediated reduction in the $Hys_{(V)}$'s area of I_h. Yohimbine is an antagonist of α-adrenergic receptors. As such, the inhibition of I_h's $Hys_{(V)}$ caused by dexmedetomidine is not associated with a mechanism highly linked to its interaction with α_2-adrenergic receptors, although pituitary cells were previously demonstrated to express those receptors [16]. It has been reported that HCN2, HCN3, or mixed HCN2+HCN3 channels are intrinsically expressed in GH_3 cells or other types of endocrine or neuroendocrine cells [4,5,17,18]. Because of the importance of I_h (i.e., HCNx-encoded currents) in contributing to the excitability and automaticity in different excitable cells [3,4,7,17,18], findings from this study could provide additional but important insights into electrophysiological and pharmacological properties of dexmedetomidine or other structurally similar compounds (e.g., medetomidine). Dexmedetomidine that viably and directly targets ionic channels [15,19] is therefore expected to have a significant therapeutic potential. However, whether dexmedetomidine-induced bradycardia or different cardioprotective action [20] is pertinent to its inhibitory effect on the magnitude and $Hys_{(V)}$ of I_h intrinsically in heart cells warrants further investigations.

2.3. Oxaliplatin

Oxaliplatin (Eloxatin®) belongs to a family of platinum-based chemotherapeutic compounds. Despite the fair safety profile,prolong treatment of oxaliplatin could induce severe peripheral neuropathy, affecting sensory and motor nerve fibers [21–25]. In agreement with previous observations [26,27], the I_h natively existing in GH_3 cells was demonstrated to undergo either a $Hys_{(V)}$ change, or a mode shift in situations where the voltage sensitivity in gating charge movements of the current depends on the previous state of the channel [7,11,12]. Recent investigations have clearly demonstrated that the presence of oxaliplatin was capable of enlarging such $Hys_{(V)}$'s Δarea involved in the voltage-dependent elicitation of I_h [11]. Furthermore, subsequent addition of ivabradine, but still in the continued presence of oxaliplatin, could attenuate oxaliplatin-mediated increase in the Δarea of $Hys_{(V)}$ in response to triangular V_{ramp} [11]. Ivabradine has been reported to be an inhibitor of I_h [18,28–30]. Therefore, the oxaliplatin actions occurring in vivo are not exclusively connected to the formation of platinum-DNA adducts. The perturbations by oxaliplatin on $Hys_{(V)}$ change of I_h is thus another intriguing mechanism, through which it or other structurally related compounds can interfere with cell behaviors, particularly in electrically excitable cells [21–23,25].

2.4. Honokiol

Honokiol, a hydroxylated biphenyl compound obtained from *Magnolia officinalis* and from other species of the family Magnoliaceae, has been used in traditional Asian medicine [31]. In a recent study, the authors exploited a long-lasting triangular V_{ramp} for the measurement of the $Hys_{(V)}$ properties in I_h. In this study, as whole-cell configuration

was achieved, it is clear that the trajectory of I_h in response to the upsloping (i.e., depolarizing from −150 to x40 mV) and downsloping (hyperpolarizing from −40 to −150 mV) V_{ramp} as a function of time was distinguishable between these two limbs of triangular V_{ramp} [11,12,26,32]. Importantly, honokiol was capable of diminishing $Hys_{(V)}$'s strength involved in the voltage-dependent activation of I_h. Moreover, with the continued presence of honokiol, the further application oxaliplatin could attenuate honokiol-mediated decrease of the Δarea of the $Hys_{(V)}$ in response to triangular V_{ramp}. Oxaliplatin was previously reported to enhance the $Hys_{(V)}$ strength of I_h [11,12,30]. However, although the voltage ranges in which I_h activation occurs, either in control conditions or after the honokiol treatment, appear to fall outside of the values of the membrane in a neuron, it needs to be noted that a small fraction of I_h is tonically activated at rest [33]. Moreover, since the macroscopic I_h in GH_3 cells could be a mixture of several channel currents (i.e., HCNx-encoded current), whether honokiol can affect either I_h existing in a variety of cells or different types of I_h remains to be rigorously evaluated. The extent to which the honokiol-induced inhibition of I_h along with its perturbations on $Hys_{(V)}$ contributes to anti-inflammatory or antinociceptive action [25,34,35] is yet to be explored.

2.5. Lutein (Xanthophyll, β,ε-Carotene-3,3′-Diol or 3,3′-Di-Hydroxy-β,α-Carotene)

The $Hys_{(V)}$ properties of I_h activated by triangular Vramp were known to perturb the electrical behaviors of various excitable cells [6,26,30]. Voltage-sensing domain relaxation in the channel proteins (e.g., HCNx channels) has been noticed to involve in such $Hys_{(V)}$ behavior [26,36]. Alternatively, the observed "inertia" in the responsiveness of HCNx channels can be driven by changes in their electrical sensitivity, which is presumably allowed to resemble that occurring in ferromagnetic materials displaying $Hys_{(V)}$ behaviors [1,2]. Of notice, the I_h intrinsically residing in GH_3 cells underwent a non-equilibrium property of instantaneous I_h. That is, there appears to be an anti-clockwise $Hys_{(V)}$ loop responding to the isosceles-triangular Vramp as demonstrated in Figure 1A. Such perturbations have been viewed to be dynamically linked to a mode shift in situations where the voltage sensitivity of gating charge movements (i.e., voltage-sensing domain relaxation) depends on the previous state (or conformation) of the channel (e.g., HCNx channel). Of additional interest, GH_3-cell exposure to lutein resulted in a significant reduction in $Hys_{(V)}$ strength of I_h evoked by long-lasting inverted triangular Vramp (Figure 1A,B). Upon continued exposure to lutein (3 μM), the subsequent addition of oxaliplatin (10 μM) was able to attenuate lutein-mediated decrease in the Δarea of I_h's $Hys_{(V)}$ observed in these cells. Oxaliplatin, a platinum-based anti-neoplastic agent, has been demonstrated to be an activator of I_h [11,23]. The presence of lutein effectively suppressed the magnitude of I_h in pituitary GH_3 cells with an IC_{50} value of 4.1 μM. Under current-clamp potential recordings, the sag potential evoked by long-lasting hyperpolarizing current stimulus also became reduced during cell exposure to this compound [37]. Lutein is one of the few xanthophyll carotenoids which exist not only in vegetables and fruits, but is also enriched in the macular of the human retina [38].

Moreover, based on the docking prediction, it is likely that the interaction of the lutein molecules with HCN channels could be located at the cytosolic side of the membrane [37]. Lutein may thus bind to the HCNx channels and interfere with channel gating to alter the magnitude, gating and $Hys_{(V)}$ of I_h. Findings from these recent reports tempt us to propose that the I_h present in different cell types could thus be unidentified, but the lutein molecules can act through distinctive targets to affect the functional activities of the cells involved. Nonetheless, lutein-mediated decrease in the $Hys_{(V)}$'s area is thought to be strongly linked to the voltage-dependent elicitation of HCN channel [7,27,36]. However, either whether the lutein molecules can interact mainly with the voltage-sensing domains of HCNx channels [7] to alter $Hys_{(V)}$ strength of the channel, or how lutein-mediated changes in the $Hys_{(V)}$'s strength influence the functional activities (e.g., electrical behaviors) in variable excitable cells, still remains to be explored.

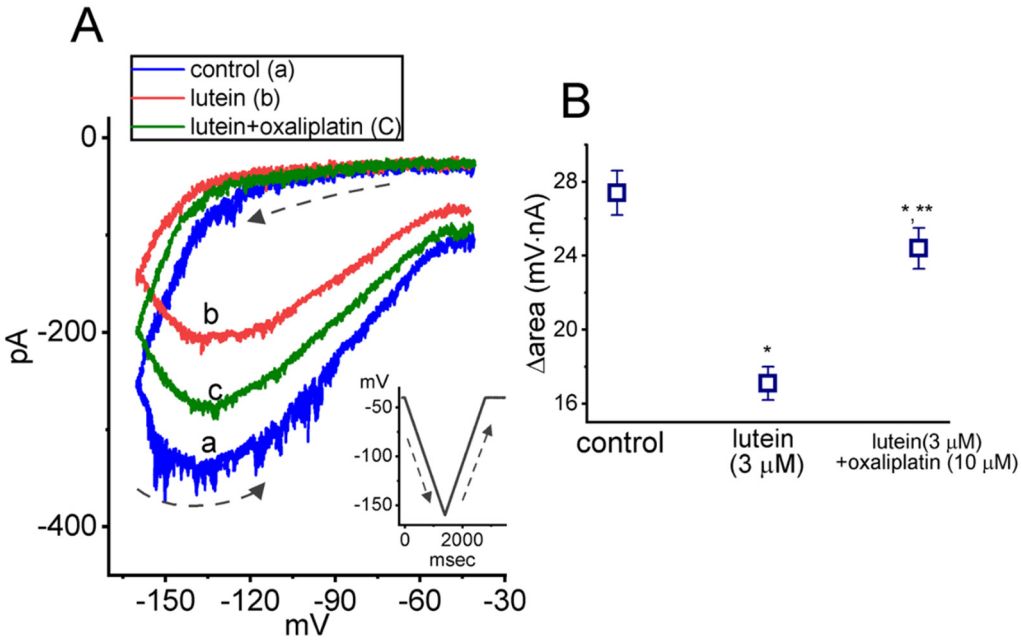

Figure 1. Effect of lutein and lutein plus oxaliplatin on $Hys_{(V)}$ of I_h measured from pituitary GH_3 cells. The experiments were conducted in cells bathed in Ca^{2+}-free Tyrode's solution, and the recording pipette was filled up with K^+-containing solution. The tested cell was held at −40 mV and the inverted isosceles-triangular V_{ramp} from −40 to −150 mV with a duration of 3.2 s (or ramp speed of ±69 mV/s) was thereafter applied to evoke I_h's $Hys_{(V)}$. (**A**) Representative $Hys_{(V)}$'s traces of I_h (i.e., the relation of forward [descending] or backward [ascending] current versus membrane potential). a: control (blue color); b: 3 μM lutein (red color); and c: 3 μM lutein plus 10 μM oxaliplatin (green color). Inset indicates the voltage protocol imposed. The black dashed arrows underneath the current traces in the control period (i.e., neither lutein nor oxaliplatin was present) indicate I_h trajectory in an anti-clockwise direction when time passes during the inverted triangular V_{ramp}. (**B**) Summary graph disclosing effects of lutein (3 μM) and lutein (3 μM) plus oxaliplatin (10 μM) on the Δarea of I_h's $Hys_{(V)}$ (i.e., the curves encircled by I_h's $Hys_{(V)}$ activated during the descending and ascending limb of the triangular V_{ramp}). * Significantly different from control ($p < 0.05$) and ** significantly different from lutein (3 μM) alone group ($p < 0.05$).

Additionally, HCN channels have been previously demonstrated to be linked to phototransduction in photosensitive retinal ganglion cells [39]. Its activity was found either to alter the electroretinographic ON and OFF responses or to delay photoreceptor degeneration [40]. To what extent lutein-mediated changes in $Hys_{(V)}$ behavior of I_h is associated with its action on age-related diseases (e.g., macular degeneration) [41] still needs to be further determined.

3. $Hys_{(V)}$ Behavior Residing in *Erg*-Mediated K^+ Current ($I_{K(erg)}$)

3.1. UCL-2077 (3-(Triphenylmethylaminomethyl)pyridine))

The $I_{K(erg)}$ encoded by three different subfamilies of the gene KCNH is known to give rise to the pore-forming α-subunit of erg-mediated K^+ (i.e., K_{erg} or K_V11) channels. These macroscopic currents are regarded to constitute the cloned counterpart of the rapidly activating delayed-rectifying K^+ currents in heart cells, where the KCNH2 gene encodes the pore-forming α-subunit of the $K_V11.1$ channels, commonly identified as hERG [42,43]. These currents inherently existing in neurons or in different types of electrically excitable cells, such as endocrine or neuroendocrine cells, can highly influence the maintenance of the resting potential as well as the increase in subthreshold excitability [44,45]. In GH_3 cells bathed in Ca^{2+}-free high-K^+ solution, as whole-cell configuration in the patch-clamp current recordings was established, the examined cell was hyperpolarized from −10 to

long-lasting hyperpolarization (e.g., 1 s) and the deactivating $I_{K(erg)}$ with a slowly decaying time course can be robustly elicited [30,44,46]. Moreover, the $Hys_{(V)}$ properties present in $I_{K(erg)}$ have been proposed to play a role in influencing the electrical behavior of excitable cells. In an earlier study, consistent with previous observations in HCN channels [26,27,36], K_{erg} channels inherently existing in GH_3 cells were noticed to undergo either a $Hys_{(V)}$ in their voltage dependence or a mode-shift, in which the voltage sensitivity of gating charge movements depends on the previous state [47,48]. The $I_{K(erg)}$'s $Hys_{(V)}$ reflects that a mode shift during channel activation may exist because the voltage sensitivity of the gating charge movement depends on the previous state (conformation) of K_{erg} channels. Under such a scenario, when the membrane potential becomes negative (i.e., the downward limb of the inverted triangular V_{ramp}), the voltage dependence of K_{erg} channel may shift the mode of $Hys_{(V)}$ to one which occurs at more negative potentials, thereby leading to an increase in membrane repolarization. However, as the membrane potential is depolarized (i.e., during initiation of action potentials or upward end of the triangular V_{ramp}), the voltage-dependence of $I_{K(erg)}$ activation would quickly switch to less depolarized voltages with a smaller current magnitude, thereby having the tendency to increase membrane excitability [47]. The experimental results also revealed that the presence of UCL-2077 was able to decrease $Hys_{(V)}$'s strength of I_h elicitation by triangular V_{ramp} [48]. Although the underlying mechanism of neuronal slow after-hyperpolarization is currently unclear, previous studies demonstrated that the ability of UCL-2077 in slow modification after-hyperpolarization [49] could be, partly if not entirely, attributed to its modifications on the magnitude, gating kinetics, and $Hys_{(V)}$ behavior of V_{ramp}-induced $I_{K(erg)}$.

3.2. SM-102 (1-Octylnonyl 8-[(2-Hydroxyethyl)[6-oxo-6(Undecyloxy)hexyl]amino]-Octanoate)

SM-102 is a synthetic and ionizable amino lipid that has been widely used in combination with other lipids in the formation of lipid nanoparticles [50–52]. Formulations containing SM-102 have been noticeably used in the development of lipid nanoparticles for the delivery of mRNA-based vaccines. For example, SM-102 is known to be one of the ingredients in the Moderna™ COVID-19 vaccine [52]. Recent investigations have also disclosed that the strength of $Hys_{(V)}$ of $I_{K(erg)}$ elicited by the upright isosceles-triangular V_{ramp} was profoundly decreased as cells were exposed to SM-102 or TurboFectin™ [53]. TurboFectin™ is a proprietary mixture of a broad-spectrum protein/polyamine with histones and lipids, which is known to be a transfection reagent. Moreover, with continued exposure to SM-102 or TurboFectin™, further application of PD118057 was able to attenuate the inhibition by these two agents on $I_{K(erg)}$'s strength activated during the triangular V_{ramp}. PD118057 was previously reported to be an activator of $I_{K(erg)}$ [54]. The magnitude of inwardly rectifier K^+ currents inherently in BV2 microglial cells was also subjected to be inhibited by SM-102. In sum, SM-102 concentration-dependently suppressed $I_{K(erg)}$ magnitude in endocrine cells (e.g., GH_3 or MA-10 cells) along with the decrease of $Hys_{(V)}$'s strength of the current [53]. These above actions are thus anticipated to contribute to their functional effects on different cell types, presumably similarly affected in vitro or in vivo.

3.3. Isoplumbagin (5-Hydroxy-3-Methyl-1,4-Naphthoquinone) and Plumbagin (5-Hydroxy-2-Methyl-1,4-Naphthoquinone)

Isoplumbagin is a naturally occurring quinone from *Lawsonia inermis* or *Plumbago europaea*, while plumbagin, another hystodyl-1,4-naphthoquinone, is an alkaloid obtained from the roots of the plants of the Plumbago genus. Isoplumbagin and plumbagin have recently been demonstrated to exert anti-neoplastic activity against an array of cancers [55,56]. Earlier studies have revealed that the $I_{K(erg)}$ residing in GH_3 cells did undergo $Hys_{(V)}$ behavior activated during the inverted isosceles-triangular V_{ramp}, reflecting that the K_{erg} channels in these cells display a clear $Hys_{(V)}$ in the voltage dependence, which is closely linked to the voltage sensor domain inherently in the channel [48,53,57]. Moreover, upon cell exposure to isoplumbagin or plumbagin, the Δarea (i.e., the area encircled by the $Hys_{(V)}$ curves elicited by the descending and ascending direction) of $I_{K(erg)}$'s $Hys_{(V)}$ during the in-

verted triangular V_{ramp} was markedly reduced [57]. Isoplumbagin was also demonstrated to suppress $I_{K(erg)}$ magnitude in MA-10 Leydig tumor cells [57]. Therefore, the inhibition by isoplumbagin or plumbagin of $I_{K(erg)}$'s magnitude and $Hys_{(V)}$'s strength would be expected to have an important impact on the discharge patterns of actions potentials occurring in excitable cells. Docking results have additionally shown that there appears to be a predicted interaction (i.e., the formation of hydrogen bond and hydrophobic contacts) between the isoplumbagin or plumbagin molecule and hERG channel [57]. In this regard, isoplumbagin, plumbagin, or other structurally similar compounds [58] could be intriguing compounds useful for characterizing the K_{erg} channels. Moreover, it remains to be studied whether this ionic mechanism of their actions on $I_{K(erg)}$ described presently can be closely linked to their actions on either functional activities or aberrant growth of different neoplastic cells [59,60].

4. $Hys_{(V)}$ Behavior Residing in M-Type K^+ Current ($I_{K(M)}$)

4.1. Remdesivir (Development Code: GS-5734)

It has been shown that the KCNQ2, KCNQ3, or KCNQ5 encodes the core subunit of $K_V7.2$, $K_V7.3$, or $K_V7.5$ channels. The enhanced activity of this family of K^+ channels (KCNQx, K_V7x, or K_M [M-type K^+] channels) can generate macroscopic M-type K^+ current ($I_{K(M)}$) [30,61–63]. Once evoked during membrane depolarization, the currents have been disclosed to exhibit a slowly activating and deactivating property as well as to affect the bursting patterns in different types of neurons, endocrine and neuroendocrine cells [30,63–65]. Remdesivir, a broad-spectrum antiviral agent, is recognized as a monophosphoramidate prodrug of an adenosine analog that metabolizes into its active form GS-441524 which is a C-adenosine nucleoside analog [66]. This compound, a nucleotide-analog inhibitor of RNA-dependent RNA polymerase, is thought to be highly active against coronaviruses (CoVs), including MERS-Cov and SARS CoV-2 [67]. The recent investigations have disclosed that remdesivir could suppressed the magnitude of $I_{K(M)}$ in pituitary GH_3 cells [68]. Moreover, the magnitude of $I_{K(M)}$'s $Hys_{(V)}$ elicited by long-lasting triangular V_{ramp} was diminished by adding remdesivir. In Jurkat T-lymphocytes, remdesivir could effectively decrease the amplitude of delayed-rectifier K^+ current concomitantly with the raised rate of current inactivation evoked by step depolarization. As such, in terms of the remdesivir molecule itself, there seems to be an unintentional activity of the prodrug on $I_{K(M)}$. The perturbing effects of remdesivir on membrane ionic currents were noted to be rapid in onset, and they should be upstream of its actions occurring inside the cytosol or nucleus. Its inhibition of $I_{K(M)}$'s $Hys_{(V)}$ emerging in a non-genomic fashion might provide additional but important mechanisms through which in vivo cellular functions are perturbed.

4.2. QO-58 (5-(2,6-Dichloro-5-Fluoropyridin-3-yl)-3-Phenyl-2-(Trifluoromethyl)-1H-Pyrazolol[1,5-a]pyrimidin-7-One)

The $Hys_{(V)}$ behavior of ionic currents has been recently noticed to exert important impacts on electrical behaviors of action potential firing [26,27,62,63]. The $I_{K(M)}$ intrinsically residing in GH_3 cells was robustly observed to undergo V_{ramp}-induced $Hys_{(V)}$ [65], suggesting that the voltage sensitivity of gating charge movements relies on the previous state (or conformation) of the M-type K^+ (K_M) channel. Alternatively, as the membrane potential of the cell becomes depolarized (i.e., during initiation of an action potential or the upsloping limb of the triangular V_{ramp}), the voltage dependence of $I_{K(M)}$ activation would switch to less depolarized voltage with a small current magnitude, thereby causing the depression of membrane excitability. However, as the membrane potential becomes negative (i.e., downward V_{ramp}), the voltage dependence of K_M channels may shift the mode of $Hys_{(V)}$ to one which occurs at more negative potentials, thereby resulting in an increase in membrane repolarization. Moreover, upon triangular V_{ramp} with varying durations, QO-58 increased the $Hys_{(V)}$'s strength of $I_{K(M)}$ [65]. QO-58 has been demonstrated previously to be an opener of KCNQx (K_V7x) channels [65,69,70]. In this regard, the experimental observations led to the notion that there would be a perturbing stimulatory effect of QO-58 on such

non-equilibrium property (i.e., non-linear $Hys_{(V)}$ behavior) in K_M (or K_V7) channels in electrically excitable cells. However, how QO-58-induced modifications on $I_{K(M)}$'s $Hys_{(V)}$ are linked to the behavior of these cells occurring in vivo remains to be further resolved.

5. $Hys_{(V)}$ Behavior Residing in L-Type Ca^{2+} Current ($I_{Ca,L}$)

Zingerone (Ginerone, Vanillylacetone)

Zingerone is a nontoxic methoxyphenol isolated from the rhizome of ginger (*Zingiber officinale* Roscoe), and it has been used as a flavor additive in spiced oils and in perfumery to introduce exotic aromas. It is widely viewed to have potential anti-inflammatory, antidiabetic, antilipolytic, antidiarrheal, antispasmodic, and anti-tumor properties [71]. In a recent study, pituitary GH_3 cells were kept in normal Tyrode's solution containing 1.8 mM $CaCl_2$, and when an abrupt double V_{ramp} was applied to the tested cell, there appeared a $Hys_{(V)}$ loop with a figure-of-eight pattern of L-type Ca^{2+} current ($I_{Ca,L}$) [72]. The $Hys_{(V)}$ properties of $I_{Ca,L}$ are noted to be distinguishable from those described above in either I_h, $I_{K(erg)}$ or $I_{K(M)}$ evoked by triangular V_{ramp}. In other words, the trajectory of the instantaneous current induced by V_{ramp} revealed two loops, namely, a high-threshold anticlockwise and a low-threshold clockwise loop, during $Hys_{(V)}$ elicitation. However, as extracellular Ca^{2+} was replaced with Ba^{2+} ions, the low-threshold current at the downsloping phase of triangular V_{ramp} diminished, whereas the high-threshold current at the upsloping end of V_{ramp} became increased. The formation of a low-threshold clockwise loop was thought to be attributed either to the magnitude of the Ca^{2+}-activated nonselective cationic currents or the late component of $I_{Ca,L}$ [73,74]. Consequently, the replacement of Ca^{2+} ions with Ba^{2+} ions increased the amplitude of $I_{Ca,L}$ (i.e., barium inward current, I_{Ba}) activated by rectangular depolarization from −50 to +10 mV, in combination with a conceivable slowing in inactivation process of the current. However, the $Hys_{(V)}$ of the current activated by the double V_{ramp} was reduced during the high-amplitude loop of V_{ramp}, as well as it was concurrently increased at the low-amplitude loop [72]. Of additional note, as cells were exposed to zingerone, the area (encircled by $I_{Ca,L}$'s $Hys_{(V)}$) of both high- and low-threshold loop of $I_{Ca,L}$ activated by the V_{ramp} were markedly reduced. Whether zingerone-mediated inhibition of $I_{Ca,L}$ accompanied by the decreased $Hys_{(V)}$ strength of the current can be responsible for its potential to attenuate seizure activity [75,76], remains to be further evaluated.

6. $Hys_{(V)}$ Behavior Residing in Persistent Na^+ Current ($I_{Na(P)}$)

6.1. Esaxerenone (Minnebro®)

Esaxerenone, known to be a newly oral, non-steroidal selective blocker on the activity of mineralocorticoid receptor, has been growingly used for the management of various pathological disorders, such as primary aldosteronism, refractory hypertension, chronic kidney disease, diabetic nephropathy, and heart failure [77–79]. In a recent investigation, the addition of esaxerenone to pituitary GH_3 cells suppressed the transient ($I_{Na(T)}$) and late component ($I_{Na(L)}$) of I_{Na} with effective IC_{50} of 13.2 and 3.2 μM, respectively [80]. Furthermore, the non-linear $Hys_{(V)}$ of V_{ramp}-induced $I_{Na(P)}$ in the control period (i.e., neither tefluthrin nor esaxerenone was present) and during cell exposure to tefluthrin or tefluthrin plus esaxerenone was observed by the upright isosceles-triangular V_{ramp} with varying durations. In particular, when cells were exposed to 10 μM tefluthrin, the peak $I_{Na(P)}$ amplitude activated at the forward (upsloping) limb of the triangular V_{ramp} was noted to increase, particularly at the level of −30 mV, whereas the $I_{Na(P)}$ amplitude at the backward (downsloping) end at −80 mV arose. In this regard, distinguishable from $Hys_{(V)}$ configuration present in I_h, $I_{K(erg)}$ and $I_{K(M)}$ elaborated above, the instantaneous figure-of-eight (i.e., infinity-shaped: ∞) configuration residing in the I_h's $Hys_{(V)}$ loop during upright triangular V_{ramp} appeared. These results indicate that, as the time goes by during activation, there is a counterclockwise direction in the high-threshold loop (i.e., the relationship of current amplitude as a function of membrane potential), followed by a clockwise direction in the low-threshold loop. Consequently, in the presence of 10 μM

tefluthrin, the figure-of-eight configuration in the $Hys_{(V)}$ loop elicited by the triangular V_{ramp} was demonstrated and further enhanced. Tefluthrin, a type-I pyrethroid insecticide, has been previously demonstrated to be an activator of I_{Na} accompanied by the slowed inactivation of the current [81–83]. In other words, there appeared to be the two distinct types of $I_{Na(P)}$, i.e., low-threshold (i.e., activating at a voltage range near the resting potential of the cell) and high-threshold loop (i.e., activating at a voltage range near the maximal I_{Na} achieved), clearly observed ruing cell exposure to tefluthrin. Of note, the low-threshold $I_{Na(P)}$ was identified to be activated (at the voltage range near the resting potential) upon the downsloping end of the triangular ramp pulse. However, the high-threshold $I_{Na(P)}$ (at the voltage range where peak $I_{Na(T)}$ was maximally activated) was by the upsloping end of such V_{ramp}. As the ramp speed decreased with a lowering in peak V_{ramp}, the area of such $Hys_{(V)}$ became progressively reduced. Therefore, finding from these results revealed that the $I_{Na(P)}$ elicited by triangular V_{ramp} was observed to undergo $Hys_{(V)}$ changes in the voltage-dependence found in GH_3 cells [80].

In an earlier study, as GH_3 cells were exposed to tefluthrin, the voltage-dependent movement of S4 segment residing in Na_V channels could be perturbed; as a result, the coupling of the pore domain to the voltage-sensor domain was enhanced [83]. Such unique type of $Hys_{(V)}$ behavior inherently in Na_V channels would potentially play substantial role either in influencing electrical behaviors, Na^+ overload due to an excessive Na^+ influx, or in hormonal secretion in various types of excitable cells during exposure to pyrethroid insecticides (e.g., tefluthrin or other structurally similar synthetic pyrethroids [e.g., deltamethrin, metofluthrin, and permethrin]). Additionally, the subsequent addition of esaxerenone, but still during continued exposure to tefluthrin, was noted to result in a marked attenuation of $Hys_{(V)}$ strength responding to triangular V_{ramp} [80]. The results presented herein are interesting, and they hence led us to propose that, in concert with its antagonistic action of mineralocorticoid receptor, the exposure to esaxerenone may directly modify the magnitude, gating properties, and $Hys_{(V)}$ strength of I_{Na} present in different excitable cells. It also needs to be mentioned that the activity of Na_V channels has been found to be functionally expressed in various types of vascular smooth muscles [84,85]. Therefore, it is worth pursuing to a further extent as to which esaxerenone-induced antihypertensive action [78,79] is associated with its additional inhibitory action on I_{Na} (i.e., $Na_V1.7$-encoded current) inherently in vascular smooth myocytes.

In this study, we also explored how the protein of the $hNa_V1.7$ channel could be optimally docked with the tefluthrin molecule by using PyRx software. The protein structure of $hNa_V1.7$ was obtained from RCB PDB (ID: 5EK0) [86]. The predicted docking sites of the tefluthrin molecule with which the amino acid residues can interact are presented in Figure 2. It is thus important to note that the tefluthrin molecule may form hydrophobic contacts with certain amino-acid residues, including Thr1678(B), Leu1679(A), Leu1679(C), Leu1679(D), Glu1680(D), Ser1681(D), and Px41804(B) (what is this?). The atom in the tefluthrin molecule has a hydrogen bond with residue Thr1709(C) at a distance of 3.23 Å. On the basis of the $Na_V1.7$ [Antrozous pallidus] protein sequence (GenBank: ASY-04966.1, https://www.ncbi.nlm.nih.gov/protein/ASY04966.1?report=gpwithparts&log$=seqview, accessed on 21 August 2022), the inactivation gate of the channel is found to be located at the residue positions ranging between 1459 and 1462, which are adjacent to the docking sites of the tefluthrin molecule. These docking results therefore tempted us to propose that the tefluthrin molecule can dock to the transmembrane segment (position: 1665–1683) of $hNa_V1.7$ channel (PDB: 5EK0) with a binding affinity of −7.5 kcal/mol, thereby potentially influencing the magnitude, gating kinetics, and $Hys_{(V)}$ strength of I_{Na}.

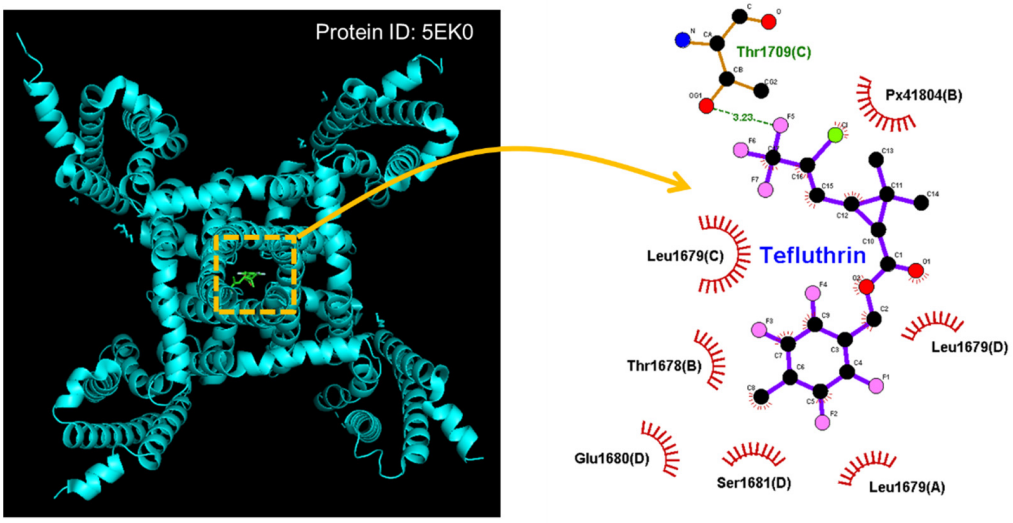

Figure 2. Docking results of the hNa$_V$1.7 channel and the tefluthrin molecule. The protein structure of hNa$_V$1.7 was acquired from RCB PDB (ID: 5EK0), whereas the chemical structure of tefluthrin was from PubChem (compound CID: 5281874 [3D conformer]). The structure of the hNa$_V$1.7 channel was docked by the tefluthrin molecule in PyRx software (http://pyrx.sourceforge.io/) (accessed on 26 July 2022). Diagram of the interaction between the hNa$_V$1.7 channel and the tefluthrin molecule generated by LigPlot$^+$ (http://www.ebi.ac.uk/thornton-srv/software/LIGPLOT/) (accessed on 26 July 2022). Note that the red arcs on which spokes faced radiating toward the ligand (i.e., tefluthrin) represent hydrophobic interactions, while green dotted line residing in amino-acid residue (i.e., Thr1708(C)) is the formation of a hydrogen bond.

6.2. Mirogabalin

Mirogabalin (Tarlige®) is an orally administered gabapentinoid, and it was thought to be a selective ligand for the $\alpha_2\delta$-1 subunit of voltage-gated Ca^{2+} channels [87]. More notable than the issue concerning the magnitude of mirogabalin-induced reduction in I_{Na}, is the current observation of the non-linear Hys$_{(V)}$ of $I_{Na(P)}$ elicited by using the upright isosceles-triangular V_{ramp} in pituitary GH$_3$ lactotrophs [88]. The presence of mirogabalin in GH$_3$ cells caused a concentration-dependent inhibition of $I_{Na(T)}$ and $I_{Na(L)}$ amplitude with the estimated IC_{50} value of 19.5 and 7.3 μM, respectively [88]. Moreover, during cell exposure to mirogabalin, the peak $I_{Na(P)}$ activated by the ascending (upsloping) limb of the triangular V_{ramp} became decreased, particularly at the level of −10 mV, while the $I_{Na(P)}$ amplitude at the descending (downsloping) phase was also concurrently reduced at the level of −80 mV. As a result, there turned out to be two distinct types of Hys$_{(V)}$ loop; that is, a high-threshold loop with a peak at −10 mV (i.e., activating at a voltage range near the maximal amplitude of transient Na^+ current ($I_{Na(T)}$ evoked by brief step depolarization), and a low-threshold loop with a peak at −80 mV (i.e., activating at a voltage near the resting membrane potential). The application of mirogabalin was able to attenuate the Hys$_{(V)}$ strength of $I_{Na(P)}$ effectively [88]. Under this scenario, the observations reveal that the triangular V_{ramp}-induced $I_{Na(P)}$ undergoes striking Hys$_{(V)}$ behavior with the voltage dependence, and that such Hys$_{(V)}$ loops responding to triangular V_{ramp} are subjected to attenuation by adding mirogabalin. The Hys$_{(V)}$ behavior of $I_{Na(P)}$ existing in endocrine or neuroendocrine cells in vivo could be strongly linked to the magnitude of Na^+ background currents, as reported previously [17,27,82,89–95]. Alternatively, genetic defects (i.e., gain-of-function) in Na$_V$ channel inactivation that led to small, sustained $I_{Na(P)}$, are recognized to have devastating consequences, including neuropathic pain and convulsant activity [89,90,94,96–98].

6.3. Dapagliflozin (Foxiga®)

Dapagliflozin is viewed to be a selective inhibitor of Na^+-dependent glucose co-transporter (SGLT) that can block glucose transport which is highly selective for SGLT2 over SGLT1 [99–101]. However, an earlier report has shown the capability of empagliflozin, another structurally similar compound, in blocking cardiac late Na^+ currents [102]. Of additional notice, the recent observations at our laboratory found that further application of dapagliflozin (10 μM) in the presence of tefluthrin (10 μM) could effectively and directly attenuate dapagliflozin-enhanced strength of $I_{Na(P)}$'s $Hys_{(V)}$ observed in GH_3 cells (Figure 3). Consistent with previous studies [102], dapagliflozin is effective at suppressing I_{Na} as well as at decreasing the strength of $I_{Na(P)}$'s $Hys_{(V)}$ in response to the upright isosceles-triangular V_{ramp}.

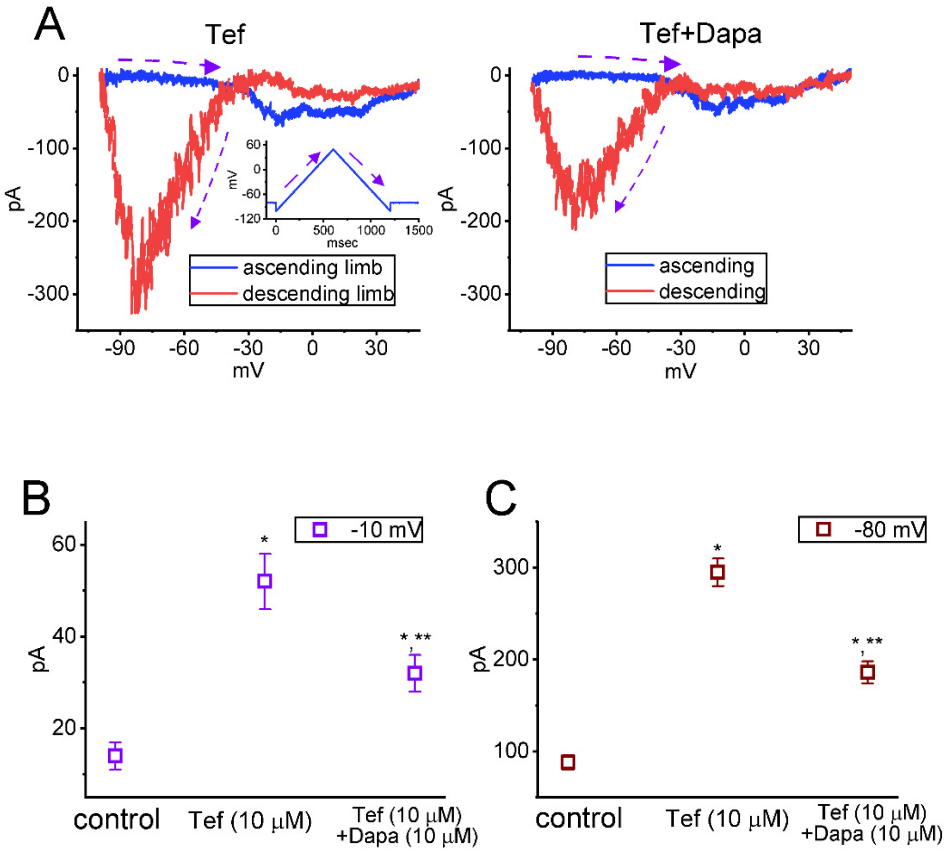

Figure 3. Effect of tefluthrin (Tef) and Tef plus dapagliflozin (Dapa) on $Hys_{(V)}$ loop of $I_{Na(P)}$ in pituitary GH_3 lactotrophs. In these experiments, we placed cells in the Ca^{2+}-free Tyrode's solution containing 10 mM tetraethylammonium chloride and 0.5 mM $CdCl_2$, and the recording electrode was filled with Cs^+-enriched solution. (**A**) Representative current traces are activated by the upright isosceles-triangular V_{ramp} for a duration of 1.2 sec, or with a ramp speed of 125 mV/s (as indicated in inset of left part). The blue color in the left and right part represents the current trace activated by the ascending (upsloping) limb of the V_{ramp}, the red color indicates the trace by the V_{ramp}'s descending (downsloping) end, and the purple dashed arrow adjacent to potential or current trace demonstrates the direction of the potential or current over which time goes during the elicitation of the long-lasting triangular V_{ramp}. Of note, there is a unique $Hys_{(V)}$ loop (i.e., the figure of eight configuration) evoked by the isosceles-triangular V_{ramp} obtained in the presence of tefluthrin (Tef, 10 μM) or tefluthrin plus dapagliflozin (Dapa, 10 μM). In (**B**,**C**), summary graphs, respectively, depict effects of Tef or Tef plus Dapa on the amplitude of $I_{Na(P)}$ activated by the upsloping (at −10 mV) and downsloping (at −80 mV) limbs of the triangular V_{ramp} (mean ± SEM; $n = 8$ for each point). * Significantly different from control ($p < 0.05$), and ** significantly from Tef (10 μM) alone group ($p < 0.05$). Of note, the magnitude appearing in (**B**,**C**) is indicated as the absolute value of current amplitude.

The effect of t-butyl hydroperoxide, a hydrophilic oxidant, on $Hys_{(V)}$ of $I_{Na(P)}$ was also further examined. As demonstrated in Figure 4, upon cell exposure to 1 mM t-butyl hydroperoxide, the $Hys_{(V)}$'s strength (at the level of −10 and −80 mV) of $I_{Na(P)}$ responding to triangular V_{ramp}. Furthermore, during the continued presence of 1 mM t-butyl hydroperoxide, further application of dapagliflozin (10 μM) was noticed to reverse t-butyl hydroperoxide-mediated increase of $Hys_{(V)}$'s strength. The results therefore reflect that, consistent with previous investigations [102], the challenge of GH_3 cells to t-butyl hydroperoxide increased $Hys_{(V)}$ magnitude of V_{ramp}-induced $I_{Na(P)}$ and the subsequent addition of dapagliflozin counteracted its increase of $Hys_{(V)}$ strength.

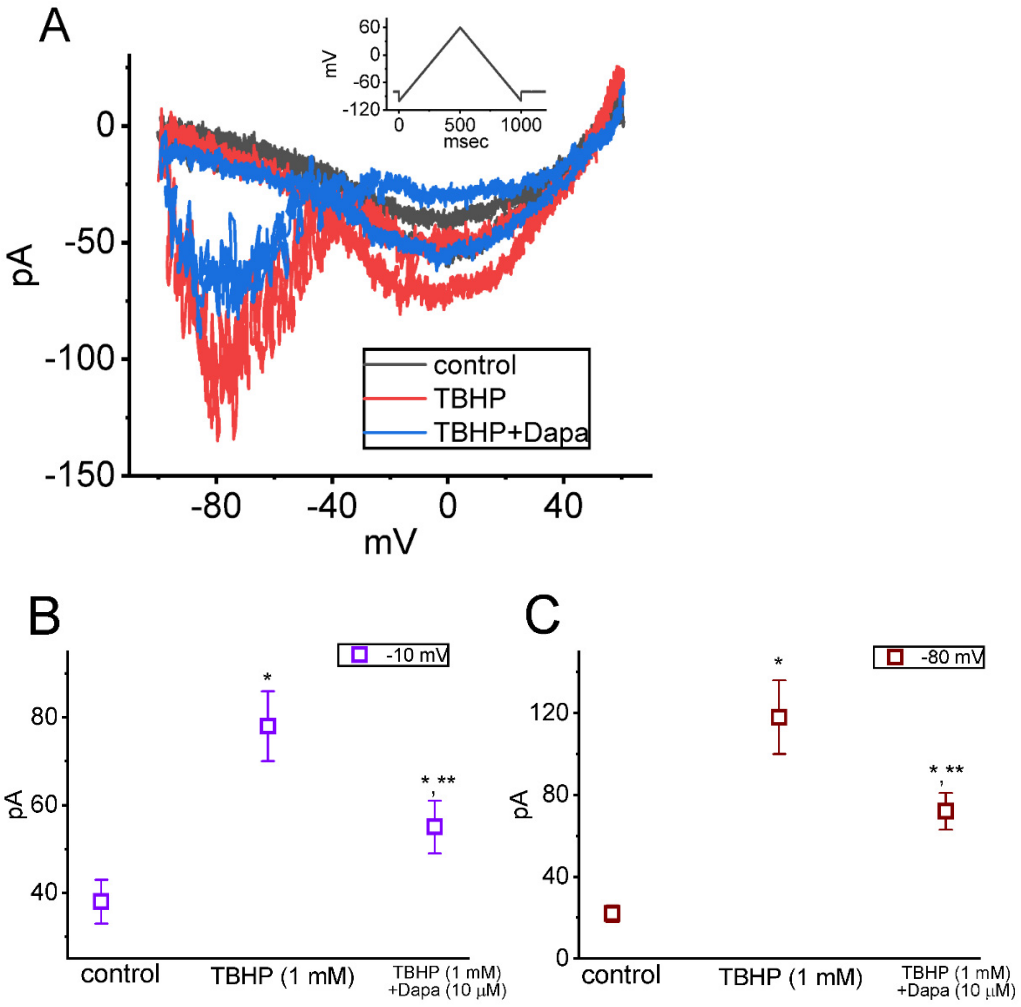

Figure 4. Effect of t-butyl hydroperoxide (TBHP) and TBHP plus dapagliflozin (Dapa) on $Hys_{(V)}$ loop of $I_{Na(P)}$ in pituitary GH_3 lactotrophs. (**A**) Representative current traces activated by the triangular V_{ramp} for a duration of 1 s (or ramp speed of 320 mV/s) (as indicated in inset). Current trace shown in black color is control (i.e., neither TBHP nor Dapa), while that in red or blue color was respectively obtained in the presence of 1 mM TBHP, or 1 mM TBHP plus 10 μM Dapa. Two red and blue traces indicate current trajectories, respectively, activated by the upsloping and downsloping end of the V_{ramp}. In (**B**,**C**), summary graphs, respectively, demonstrate effects of TBHP or TBHP plus Dapa on the amplitude of $I_{Na(P)}$ at the upsloping (−10 mV) and downsloping (−80 mV) ends of triangular V_{ramp} (mean ± SEM; n = 7 for each point). * Significantly different from control ($p < 0.05$), and ** significantly different from TBHP (1 mM) alone group ($p < 0.05$).

It has been demonstrated that the different Na_V subtypes (isoforms) can combine to constitute macroscopic I_{Na} residing in varying types of excitable cells [103,104]. $Na_V1.1$, $Na_V1.2$, $Na_V1.3$, and $Na_V1.6$ channels were previously reported to be expressed in GH_3

cells [17]. As such, distinguishable to some extent from previous reports demonstrating the ability of empagliflozin, another SGLT2 inhibitor, in inhibiting the late component of cardiac-specific Na^+ current [102], it seems unlikely that dapagliflozin-induced inhibition of I_{Na} inherently in native cells is isoform-specific. Nonetheless, the present results strongly reflect that inhibitory effect of dapagliflozin or other structurally similar compounds (e.g., canagliflozin and empagliflozin) on I_{Na}, particularly $I_{Na(P)}$, which may occur within the clinically therapeutic range, would be another obligate ionic mechanism through which they could converge to perturb the functional activities (e.g., electrical behaviors, Na^+ influx, and glucose uptake) in different excitable cells.

7. Conclusions

As described above and in published studies, the experimental observations have revealed that several voltage-gated ion channels were found to undergo non-linear $Hys_{(V)}$ behavior elicited during triangular V_{ramp}. A variety of small molecules (Table 1) known to modify the magnitude and gating of ionic currents (i.e., I_h, $I_{K(erg)}$, $I_{K(M)}$, $I_{Ca,L}$, and $I_{Na(P)}$) may pertinently perturb the $Hys_{(V)}$ behavior of the currents. The modifications of $Hys_{(V)}$ exerted by these small-molecule modulators are capable of potentially affecting the functional activities of different excitable cells, presuming that the in-vivo findings occurred.

Author Contributions: Conceptualization, S.-N.W., C.-L.W., H.-Y.C. and C.-W.C.; methodology, S.-N.W. and H.-Y.C.; software, S.-N.W. and H.-Y.C.; validation, S.-N.W. and H.-Y.C.; formal analysis, S.-N.W.; investigation, S.-N.W. and H.-Y.C.; resources, S.-N.W.; data curation, S.-N.W. and H.-Y.C.; writing—original draft preparation, S.-N.W.; writing—review and editing, S.-N.W., C.-L.W., H.-Y.C. and C.-W.C.; visualization, S.-N.W., C.-L.W., H.-Y.C. and C.-W.C.; supervision, S.-N.W., C.-L.W. and C.-W.C.; project administration, S.-N.W., C.-L.W. and C.-W.C.; funding acquisition, S.-N.W. All authors have read and agreed to the published version of the manuscript.

Funding: The research detailed in the present work was supported by grants from the Ministry of Science and Technology, Taiwan (MOST-110-2320-B-006-028 and MOST-111-2320-B-006-028). The funders in the present work are not involved in the study design, data collection, analyses, or interpretation.

Institutional Review Board Statement: Not applicable.

Informed Consent Statement: Not applicable.

Data Availability Statement: The original data is available upon reasonable request to the corresponding author.

Acknowledgments: The authors thank Tzu-Hsien Chuang for his contribution to the earlier experiments.

Conflicts of Interest: The authors declare that they have no competing interests which would prejudice its impartiality. The authors declare no conflict of interest.

Abbreviations

erg	*ether-à-go-go*-related gene
$Hys_{(V)}$	voltage-dependent hysteresis
HCN channel	hyperpolarization-activated cyclic nucleotide-gated channel
$I_{Ca,L}$	L-type Ca^{2+} current
I_h	hyperpolarization-activated cation current
$I_{K(erg)}$	*erg*-mediated K^+ current
$I_{K(M)}$	M-type K^+ current
$I_{Na(L)}$	late Na^+ current
$I_{Na(P)}$	persistent Na^+ current
$I_{Na(T)}$	transient (peak) Na^+ current
K_{erg} channel	*erg*-mediated K^+ channel
K_M channel	M-type K^+ channel
Na_V channel	voltage-gated Na^+ channel
SGLT	Na^+-dependent glucose co-transporter
V_{ramp}	ramp voltage

References

1. Krylov, D.; Velkos, G.; Chen, C.H.; Büchner, B.; Kostanyan, A.; Greber, T.; Avdoshenko, S.M.; Popov, A.A. Magnetic hysteresis and strong ferromagnetic coupling of sulfur-bridged Dy ions in clusterfullerene Dy(2)S@C(82). *Inorg. Chem. Front.* **2020**, *7*, 3521–3532. [CrossRef] [PubMed]
2. Villalba-Galea, C.A.; Chiem, A.T. Hysteretic Behavior in Voltage-Gated Channels. *Front. Pharmacol.* **2020**, *11*, 579596. [CrossRef] [PubMed]
3. Irisawa, H.; Brown, H.F.; Giles, W. Cardiac pacemaking in the sinoatrial node. *Physiol. Rev.* **1993**, *73*, 197–227. [CrossRef] [PubMed]
4. Benzoni, P.; Bertoli, G.; Giannetti, F.; Piantoni, C.; Milanesi, R.; Pecchiari, M.; Barbuti, A.; Baruscotti, M.; Bucchi, A. The funny current: Even funnier than 40 years ago. Uncanonical expression and roles of HCN/f channels all over the body. *Prog. Biophys. Mol. Biol.* **2021**, *166*, 189–204. [CrossRef]
5. Combe, C.L.; Gasparini, S. I(h) from synapses to networks: HCN channel functions and modulation in neurons. *Prog. Biophys. Mol. Biol.* **2021**, *166*, 119–132. [CrossRef]
6. Peters, C.H.; Liu, P.W.; Morotti, S.; Gantz, S.C.; Grandi, E.; Bean, B.P.; Proenza, C. Bidirectional flow of the funny current (I(f)) during the pacemaking cycle in murine sinoatrial node myocytes. *Proc. Natl. Acad. Sci. USA* **2021**, *118*, e2104668118. [CrossRef]
7. Saponaro, A.; Bauer, D.; Giese, M.H.; Swuec, P.; Porro, A.; Gasparri, F.; Sharifzadeh, A.S.; Chaves-Sanjuan, A.; Alberio, L.; Parisi, G.; et al. Gating movements and ion permeation in HCN4 pacemaker channels. *Mol. Cell* **2021**, *81*, 2929–2943.e2926. [CrossRef]
8. Depuydt, A.S.; Peigneur, S.; Tytgat, J. HCN channels in the heart. *Curr. Cardiol. Rev.* **2022**, *18*, e040222200836. [CrossRef]
9. Yavuz, M.; Aydın, B.; Çarçak, N.; Onat, F. Decreased Hyperpolarization-Activated Cyclic Nucleotide-Gated Channel 2 Activity in a Rat Model of Absence Epilepsy and the Effect of ZD7288, an Ih Inhibitor, on the Spike-and-Wave Discharges. *Pharmacology* **2022**, *107*, 227–234. [CrossRef]
10. Saito, S.; Alkhatib, A.; Kolls, J.K.; Kondoh, Y.; Lasky, J.A. Pharmacotherapy and adjunctive treatment for idiopathic pulmonary fibrosis (IPF). *J. Thorac. Dis.* **2019**, *11*, S1740–S1754. [CrossRef]
11. Chang, W.T.; Gao, Z.H.; Li, S.W.; Liu, P.Y.; Lo, Y.C.; Wu, S.N. Characterization in Dual Activation by Oxaliplatin, a Platinum-Based Chemotherapeutic Agent of Hyperpolarization-Activated Cation and Electroporation-Induced Currents. *Int. J. Mol. Sci.* **2020**, *21*, 396. [CrossRef] [PubMed]
12. Chang, W.T.; Ragazzi, E.; Liu, P.Y.; Wu, S.N. Effective block by pirfenidone, an antifibrotic pyridone compound (5-methyl-1-phenylpyridin-2[H-1]-one), on hyperpolarization-activated cation current: An additional but distinctive target. *Eur. J. Pharmacol.* **2020**, *882*, 173237. [CrossRef] [PubMed]
13. Martin, E.; Ramsay, G.; Mantz, J.; Sum-Ping, S.T. The role of the alpha2-adrenoceptor agonist dexmedetomidine in postsurgical sedation in the intensive care unit. *J. Intensive Care Med.* **2003**, *18*, 29–41. [CrossRef] [PubMed]
14. Preskorn, S.H.; Zeller, S.; Citrome, L.; Finman, J.; Goldberg, J.F.; Fava, M.; Kakar, R.; De Vivo, M.; Yocca, F.D.; Risinger, R. Effect of Sublingual Dexmedetomidine vs Placebo on Acute Agitation Associated With Bipolar Disorder: A Randomized Clinical Trial. *JAMA* **2022**, *327*, 727–736. [CrossRef] [PubMed]
15. Lu, T.L.; Lu, T.J.; Wu, S.N. Effectiveness in Block by Dexmedetomidine of Hyperpolarization-Activated Cation Current, Independent of Its Agonistic Effect on α(2)-Adrenergic Receptors. *Int. J. Mol. Sci.* **2020**, *21*, 9110. [CrossRef] [PubMed]
16. Colthorpe, K.L.; Nalliah, J.; Anderson, S.T.; Curlewis, J.D. Adrenoceptor subtype involvement in suppression of prolactin secretion by noradrenaline. *J. Neuroendocrinol.* **2000**, *12*, 297–302. [CrossRef] [PubMed]
17. Stojilkovic, S.S.; Tabak, J.; Bertram, R. Ion channels and signaling in the pituitary gland. *Endocr. Rev.* **2010**, *31*, 845–915. [CrossRef] [PubMed]
18. Spinelli, V.; Sartiani, L.; Mugelli, A.; Romanelli, M.N.; Cerbai, E. Hyperpolarization-activated cyclic-nucleotide-gated channels: Pathophysiological, developmental, and pharmacological insights into their function in cellular excitability. *Can. J. Physiol. Pharmacol.* **2018**, *96*, 977–984. [CrossRef]
19. Chen, B.S.; Peng, H.; Wu, S.N. Dexmedetomidine, an alpha2-adrenergic agonist, inhibits neuronal delayed-rectifier potassium current and sodium current. *Br. J. Anaesth.* **2009**, *103*, 244–254. [CrossRef]
20. Elliott, M.; Burnsed, J.; Heinan, K.; Letzkus, L.; Andris, R.; Fairchild, K.; Zanelli, S. Effect of dexmedetomidine on heart rate in neonates with hypoxic ischemic encephalopathy undergoing therapeutic hypothermia. *J. Neonatal. Perinatal. Med.* **2022**, *15*, 47–54. [CrossRef]
21. Hartmann, J.T.; Lipp, H.P. Toxicity of platinum compounds. *Expert Opin. Pharmacother.* **2003**, *4*, 889–901. [CrossRef]
22. Graham, J.; Mushin, M.; Kirkpatrick, P. Oxaliplatin. *Nat. Rev. Drug Discov.* **2004**, *3*, 11–12. [CrossRef]
23. Liu, X.; Zhang, L.; Jin, L.; Tan, Y.; Li, W.; Tang, J. HCN2 contributes to oxaliplatin-induced neuropathic pain through activation of the CaMKII/CREB cascade in spinal neurons. *Mol. Pain* **2018**, *14*, 1744806918778490. [CrossRef]
24. Resta, F.; Micheli, L.; Laurino, A.; Spinelli, V.; Mello, T.; Sartiani, L.; Di Cesare Mannelli, L.; Cerbai, E.; Ghelardini, C.; Romanelli, M.N.; et al. Selective HCN1 block as a strategy to control oxaliplatin-induced neuropathy. *Neuropharmacology* **2018**, *131*, 403–413. [CrossRef]
25. Yongning, Z.; Xianguang, L.; Hengling, C.; Su, C.; Fang, L.; Chenhong, L. The hyperpolarization-activated cyclic nucleotide-gated channel currents contribute to oxaliplatin-induced hyperexcitability of DRG neurons. *Somatosens. Mot. Res.* **2021**, *38*, 11–19. [CrossRef]

26. Männikkö, R.; Pandey, S.; Larsson, H.P.; Elinder, F. Hysteresis in the voltage dependence of HCN channels: Conversion between two modes affects pacemaker properties. *J. Gen. Physiol.* **2005**, *125*, 305–326. [CrossRef]
27. Fürst, O.; D'Avanzo, N. Isoform dependent regulation of human HCN channels by cholesterol. *Sci. Rep.* **2015**, *5*, 14270. [CrossRef]
28. Liu, Y.C.; Wang, Y.J.; Wu, P.Y.; Wu, S.N. Tramadol-induced block of hyperpolarization-activated cation current in rat pituitary lactotrophs. *Naunyn-Schmiedeberg's Arch. Pharmacol.* **2009**, *379*, 127–135. [CrossRef]
29. Hsiao, H.T.; Liu, Y.C.; Liu, P.Y.; Wu, S.N. Concerted suppression of I(h) and activation of I(K(M)) by ivabradine, an HCN-channel inhibitor, in pituitary cells and hippocampal neurons. *Brain Res. Bull.* **2019**, *149*, 11–20. [CrossRef]
30. Wu, S.N.; Huang, C.W. Editorial to the Special Issue "Electrophysiology". *Int. J. Mol. Sci.* **2021**, *22*, 2956. [CrossRef]
31. Bi, L.; Yu, Z.; Wu, J.; Yu, K.; Hong, G.; Lu, Z.; Gao, S. Honokiol Inhibits Constitutive and Inducible STAT3 Signaling via PU.1-Induced SHP1 Expression in Acute Myeloid Leukemia Cells. *Tohoku J. Exp. Med.* **2015**, *237*, 163–172. [CrossRef]
32. Chan, M.H.; Chen, H.H.; Lo, Y.C.; Wu, S.N. Effectiveness in the Block by Honokiol, a Dimerized Allylphenol from Magnolia Officinalis, of Hyperpolarization-Activated Cation Current and Delayed-Rectifier K(+) Current. *Int. J. Mol. Sci.* **2020**, *21*, 4260. [CrossRef]
33. Robinson, R.B.; Siegelbaum, S.A. Hyperpolarization-activated cation currents: From molecules to physiological function. *Annu Rev. Physiol.* **2003**, *65*, 453–480. [CrossRef] [PubMed]
34. Woodbury, A.; Yu, S.P.; Wei, L.; García, P. Neuro-modulating effects of honokiol: A review. *Front. Neurol.* **2013**, *4*, 130. [CrossRef] [PubMed]
35. Woodbury, A.; Yu, S.P.; Chen, D.; Gu, X.; Lee, J.H.; Zhang, J.; Espinera, A.; García, P.S.; Wei, L. Honokiol for the Treatment of Neonatal Pain and Prevention of Consequent Neurobehavioral Disorders. *J. Nat. Prod.* **2015**, *78*, 2531–2536. [CrossRef]
36. Elinder, F.; Männikkö, R.; Pandey, S.; Larsson, H.P. Mode shifts in the voltage gating of the mouse and human HCN2 and HCN4 channels. *J. Physiol.* **2006**, *575*, 417–431. [CrossRef]
37. Chuang, C.W.; Chang, K.P.; Cho, H.Y.; Chuang, T.H.; Yu, M.C.; Wu, C.L.; Wu, S.N. Characterization of Inhibitory Capability on Hyperpolarization-Activated Cation Current Caused by Lutein (β,ε-Carotene-3,3′-Diol), a Dietary Xanthophyll Carotenoid. *Int. J. Mol. Sci.* **2022**, *23*, 7186. [CrossRef]
38. Mrowicka, M.; Mrowicki, J.; Kucharska, E.; Majsterek, I. Lutein and Zeaxanthin and Their Roles in Age-Related Macular Degeneration-Neurodegenerative Disease. *Nutrients* **2022**, *14*, 827. [CrossRef]
39. Jiang, Z.; Yue, W.W.S.; Chen, L.; Sheng, Y.; Yau, K.W. Cyclic-Nucleotide- and HCN-Channel-Mediated Phototransduction in Intrinsically Photosensitive Retinal Ganglion Cells. *Cell* **2018**, *175*, 652–664.e612. [CrossRef]
40. Popova, E.; Kupenova, P. Effects of HCN channel blockade on the intensity-response function of electroretinographic ON and OFF responses in dark adapted frogs. *Acta Neurobiol. Exp.* **2020**, *80*, 192–204. [CrossRef]
41. Eisenhauer, B.; Natoli, S.; Liew, G.; Flood, V.M. Lutein and Zeaxanthin-Food Sources, Bioavailability and Dietary Variety in Age-Related Macular Degeneration Protection. *Nutrients* **2017**, *9*, 120. [CrossRef] [PubMed]
42. Vandenberg, J.I.; Perry, M.D.; Perrin, M.J.; Mann, S.A.; Ke, Y.; Hill, A.P. hERG K(+) channels: Structure, function, and clinical significance. *Physiol. Rev.* **2012**, *92*, 1393–1478. [CrossRef] [PubMed]
43. Martinson, A.S.; van Rossum, D.B.; Diatta, F.H.; Layden, M.J.; Rhodes, S.A.; Martindale, M.Q.; Jegla, T. Functional evolution of Erg potassium channel gating reveals an ancient origin for IKr. *Proc. Natl. Acad. Sci. USA* **2014**, *111*, 5712–5717. [CrossRef] [PubMed]
44. Wu, S.N.; Jan, C.R.; Li, H.F.; Chiang, H.T. Characterization of inhibition by risperidone of the inwardly rectifying K(+) current in pituitary GH(3) cells. *Neuropsychopharmacology* **2000**, *23*, 676–689. [CrossRef]
45. Matsuoka, T.; Yamasaki, M.; Abe, M.; Matsuda, Y.; Morino, H.; Kawakami, H.; Sakimura, K.; Watanabe, M.; Hashimoto, K. Kv11 (ether-à-go-go-related gene) voltage-dependent K(+) channels promote resonance and oscillation of subthreshold membrane potentials. *J. Physiol.* **2021**, *599*, 547–569. [CrossRef]
46. Chen, B.S.; Lo, Y.C.; Peng, H.; Hsu, T.I.; Wu, S.N. Effects of ranolazine, a novel anti-anginal drug, on ion currents and membrane potential in pituitary tumor GH(3) cells and NG108-15 neuronal cells. *J. Pharmacol. Sci.* **2009**, *110*, 295–305. [CrossRef]
47. Shi, Y.P.; Thouta, S.; Claydon, T.W. Modulation of hERG K(+) Channel Deactivation by Voltage Sensor Relaxation. *Front. Pharmacol.* **2020**, *11*, 139. [CrossRef]
48. Hsu, H.T.; Lo, Y.C.; Wu, S.N. Characterization of Convergent Suppression by UCL-2077 (3-(Triphenylmethylaminomethyl)pyridine), Known to Inhibit Slow Afterhyperpolarization, of erg-Mediated Potassium Currents and Intermediate-Conductance Calcium-Activated Potassium Channels. *Int. J. Mol. Sci.* **2020**, *21*, 1441. [CrossRef]
49. Zhang, L.; Kolaj, M.; Renaud, L.P. Ca^{2+}-dependent and Na+-dependent K+ conductances contribute to a slow AHP in thalamic paraventricular nucleus neurons: A novel target for orexin receptors. *J. Neurophysiol.* **2010**, *104*, 2052–2062. [CrossRef]
50. Hassett, K.J.; Benenato, K.E.; Jacquinet, E.; Lee, A.; Woods, A.; Yuzhakov, O.; Himansu, S.; Deterling, J.; Geilich, B.M.; Ketova, T.; et al. Optimization of Lipid Nanoparticles for Intramuscular Administration of mRNA Vaccines. *Mol. Ther. Nucleic. Acids* **2019**, *15*, 1–11. [CrossRef]
51. Ferraresso, F.; Strilchuk, A.W.; Juang, L.J.; Poole, L.G.; Luyendyk, J.P.; Kastrup, C.J. Comparison of DLin-MC3-DMA and ALC-0315 for siRNA Delivery to Hepatocytes and Hepatic Stellate Cells. *Mol. Pharm.* **2022**, *19*, 2175–2182. [CrossRef]
52. Ly, H.H.; Daniel, S.; Soriano, S.K.V.; Kis, Z.; Blakney, A.K. Optimization of Lipid Nanoparticles for saRNA Expression and Cellular Activation Using a Design-of-Experiment Approach. *Mol. Pharm.* **2022**, *19*, 1892–1905. [CrossRef]

53. Cho, H.Y.; Chuang, T.H.; Wu, S.N. Effective Perturbations on the Amplitude and Hysteresis of Erg-Mediated Potassium Current Caused by 1-Octylnonyl 8-[(2-hydroxyethyl)[6-oxo-6(undecyloxy)hexyl]amino]-octanoate (SM-102), a Cationic Lipid. *Biomedicines* **2021**, *9*, 1367. [CrossRef]
54. Zhou, J.; Augelli-Szafran, C.E.; Bradley, J.A.; Chen, X.; Koci, B.J.; Volberg, W.A.; Sun, Z.; Cordes, J.S. Novel potent human ether-a-go-go-related gene (hERG) potassium channel enhancers and their in vitro antiarrhythmic activity. *Mol. Pharmacol.* **2005**, *68*, 876–884. [CrossRef]
55. Srinivas, P.; Gopinath, G.; Banerji, A.; Dinakar, A.; Srinivas, G. Plumbagin induces reactive oxygen species, which mediate apoptosis in human cervical cancer cells. *Mol. Carcinog.* **2004**, *40*, 201–211. [CrossRef]
56. Liu, Y.; Cai, Y.; He, C.; Chen, M.; Li, H. Anticancer Properties and Pharmaceutical Applications of Plumbagin: A Review. *Am. J. Chin. Med.* **2017**, *45*, 423–441. [CrossRef]
57. Chen, L.; Cho, H.Y.; Chuang, T.H.; Ke, T.L.; Wu, S.N. The Effectiveness of Isoplumbagin and Plumbagin in Regulating Amplitude, Gating Kinetics, and Voltage-Dependent Hysteresis of erg-mediated K(+) Currents. *Biomedicines* **2022**, *10*, 780. [CrossRef]
58. Schulze, M.M.; Löwe, R.; Pollex, R.; Mazik, M. Structure–extractability relationships for substituted 8-hydroxyquinolines: Solvent extraction of indium ions from acidic aqueous media. *Mon. Für Chem. Chem. Mon.* **2019**, *150*, 983–990. [CrossRef]
59. Huang, M.H.; Wu, S.N.; Chen, C.P.; Shen, A.Y. Inhibition of Ca^{2+}-activated and voltage-dependent K+ currents by 2-mercaptophenyl-1,4-naphthoquinone in pituitary GH3 cells: Contribution to its antiproliferative effect. *Life Sci.* **2002**, *70*, 1185–1203. [CrossRef]
60. Tsao, Y.C.; Chang, Y.J.; Wang, C.H.; Chen, L. Discovery of Isoplumbagin as a Novel NQO1 Substrate and Anti-Cancer Quinone. *Int. J. Mol. Sci.* **2020**, *21*, 4378. [CrossRef]
61. Gribkoff, V.K. The therapeutic potential of neuronal KCNQ channel modulators. *Expert Opin. Ther. Targets* **2003**, *7*, 737–748. [CrossRef]
62. Cho, H.Y.; Chuang, T.H.; Wu, S.N. The Effectiveness in Activating M-Type K(+) Current Produced by Solifenacin ([(3R)-1-azabicyclo [2.2.2]octan-3-yl] (1S)-1-phenyl-3,4-dihydro-1H-isoquinoline-2-carboxylate): Independent of Its Antimuscarinic Action. *Int. J. Mol. Sci.* **2021**, *22*, 2399. [CrossRef]
63. Lo, Y.C.; Lin, C.L.; Fang, W.Y.; Lőrinczi, B.; Szatmári, I.; Chang, W.H.; Fülöp, F.; Wu, S.N. Effective Activation by Kynurenic Acid and Its Aminoalkylated Derivatives on M-Type K(+) Current. *Int. J. Mol. Sci.* **2021**, *22*, 1300. [CrossRef]
64. Wulfsen, I.; Hauber, H.P.; Schiemann, D.; Bauer, C.K.; Schwarz, J.R. Expression of mRNA for voltage-dependent and inward-rectifying K channels in GH3/B6 cells and rat pituitary. *J. Neuroendocrinol.* **2000**, *12*, 263–272. [CrossRef]
65. Wu, C.L.; Chuang, C.W.; Cho, H.Y.; Chuang, T.H.; Wu, S.N. The Evidence for Effective Inhibition of I(Na) Produced by Mirogabalin ((1R,5S,6S)-6-(aminomethyl)-3-ethyl-bicyclo [3.2.0] hept-3-ene-6-acetic acid), a Known Blocker of Ca(V) Channels. *Int. J. Mol. Sci.* **2022**, *23*, 3845. [CrossRef]
66. Gordon, C.J.; Tchesnokov, E.P.; Feng, J.Y.; Porter, D.P.; Götte, M. The antiviral compound remdesivir potently inhibits RNA-dependent RNA polymerase from Middle East respiratory syndrome coronavirus. *J. Biol. Chem.* **2020**, *295*, 4773–4779. [CrossRef]
67. Wang, M.; Cao, R.; Zhang, L.; Yang, X.; Liu, J.; Xu, M.; Shi, Z.; Hu, Z.; Zhong, W.; Xiao, G. Remdesivir and chloroquine effectively inhibit the recently emerged novel coronavirus (2019-nCoV) in vitro. *Cell Res.* **2020**, *30*, 269–271. [CrossRef]
68. Chang, W.T.; Liu, P.Y.; Gao, Z.H.; Lee, S.W.; Lee, W.K.; Wu, S.N. Evidence for the Effectiveness of Remdesivir (GS-5734), a Nucleoside-Analog Antiviral Drug in the Inhibition of I (K(M)) or I (K(DR)) and in the Stimulation of I (MEP). *Front. Pharmacol.* **2020**, *11*, 1091. [CrossRef] [PubMed]
69. Qi, J.; Zhang, F.; Mi, Y.; Fu, Y.; Xu, W.; Zhang, D.; Wu, Y.; Du, X.; Jia, Q.; Wang, K.; et al. Design, synthesis and biological activity of pyrazolo [1,5-a]pyrimidin-7(4H)-ones as novel Kv7/KCNQ potassium channel activators. *Eur. J. Med. Chem.* **2011**, *46*, 934–943. [CrossRef] [PubMed]
70. Zhang, F.; Mi, Y.; Qi, J.L.; Li, J.W.; Si, M.; Guan, B.C.; Du, X.N.; An, H.L.; Zhang, H.L. Modulation of K(v)7 potassium channels by a novel opener pyrazolo [1,5-a]pyrimidin-7(4H)-one compound QO-58. *Br. J. Pharmacol.* **2013**, *168*, 1030–1042. [CrossRef] [PubMed]
71. Ahmad, B.; Rehman, M.U.; Amin, I.; Arif, A.; Rasool, S.; Bhat, S.A.; Afzal, I.; Hussain, I.; Bilal, S.; Mir, M. A Review on Pharmacological Properties of Zingerone (4-(4-Hydroxy-3-methoxyphenyl)-2-butanone). *Sci. World J.* **2015**, *2015*, 816364. [CrossRef]
72. Lai, M.C.; Wu, S.N.; Huang, C.W. Zingerone Modulates Neuronal Voltage-Gated Na(+) and L-Type $Ca^{(2+)}$ Currents. *Int. J. Mol. Sci.* **2022**, *23*, 3123. [CrossRef]
73. Wu, S.N.; Li, H.F.; Jan, C.R. Regulation of Ca^{2+}-activated nonselective cationic currents in rat pituitary GH3 cells: Involvement in L-type Ca^{2+} current. *Brain Res.* **1998**, *812*, 133–141. [CrossRef]
74. Lo, Y.K.; Wu, S.N.; Lee, C.T.; Li, H.F.; Chiang, H.T. Characterization of action potential waveform-evoked L-type calcium currents in pituitary GH3 cells. *Pflugers Arch.* **2001**, *442*, 547–557. [CrossRef]
75. Simeone, K.A.; Sabesan, S.; Kim, D.Y.; Kerrigan, J.F.; Rho, J.M.; Simeone, T.A. L-Type calcium channel blockade reduces network activity in human epileptic hypothalamic hamartoma tissue. *Epilepsia* **2011**, *52*, 531–540. [CrossRef]
76. Ortner, N.J.; Striessnig, J. L-type calcium channels as drug targets in CNS disorders. *Channels* **2016**, *10*, 7–13. [CrossRef]
77. Capelli, I.; Gasperoni, L.; Ruggeri, M.; Donati, G.; Baraldi, O.; Sorrenti, G.; Caletti, M.T.; Aiello, V.; Cianciolo, G.; La Manna, G. New mineralocorticoid receptor antagonists: Update on their use in chronic kidney disease and heart failure. *J. Nephrol.* **2020**, *33*, 37–48. [CrossRef]

78. Morimoto, S.; Ichihara, A. Efficacy of esaxerenone-a nonsteroidal mineralocorticoid receptor blocker-on nocturnal hypertension. *Hypertens. Res.* **2022**, *45*, 376–377. [CrossRef]
79. Munkhjargal, U.; Fukuda, D.; Ganbaatar, B.; Suto, K.; Matsuura, T.; Ise, T.; Kusunose, K.; Yamaguchi, K.; Yagi, S.; Yamada, H.; et al. A Selective Mineralocorticoid Receptor Blocker, Esaxerenone, Attenuates Vascular Dysfunction in Diabetic C57BL/6 Mice. *J. Atheroscler. Thromb.* 2022, *online ahead of print*. [CrossRef]
80. Chang, W.T.; Wu, S.N. Characterization of Direct Perturbations on Voltage-Gated Sodium Current by Esaxerenone, a Nonsteroidal Mineralocorticoid Receptor Blocker. *Biomedicines* **2021**, *9*, 549. [CrossRef]
81. Wu, G.; Li, Q.; Liu, X.; Li-Byarlay, H.; He, B. Differential state-dependent effects of deltamethrin and tefluthrin on sodium channels in central neurons of Helicoverpa armigera. *Pestic. Biochem. Physiol.* **2021**, *175*, 104836. [CrossRef] [PubMed]
82. Wu, S.N.; Chen, B.S.; Hsu, T.I.; Peng, H.; Wu, Y.H.; Lo, Y.C. Analytical studies of rapidly inactivating and noninactivating sodium currents in differentiated NG108-15 neuronal cells. *J. Theor. Biol.* **2009**, *259*, 828–836. [CrossRef] [PubMed]
83. So, E.C.; Wu, S.N.; Lo, Y.C.; Su, K. Differential regulation of tefluthrin and telmisartan on the gating charges of I(Na) activation and inactivation as well as on resurgent and persistent I(Na) in a pituitary cell line (GH(3)). *Toxicol. Lett.* **2018**, *285*, 104–112. [CrossRef] [PubMed]
84. Saleh, S.; Yeung, S.Y.; Prestwich, S.; Pucovsky, V.; Greenwood, I. Electrophysiological and molecular identification of voltage-gated sodium channels in murine vascular myocytes. *J. Physiol.* **2005**, *568*, 155–169. [CrossRef] [PubMed]
85. Virsolvy, A.; Fort, A.; Erceau, L.; Charrabi, A.; Hayot, M.; Aimond, F.; Richard, S. Hypoxic Conditions Promote Rhythmic Contractile Oscillations Mediated by Voltage-Gated Sodium Channels Activation in Human Arteries. *Int. J. Mol. Sci.* **2021**, *22*, 2570. [CrossRef] [PubMed]
86. Ahuja, S.; Mukund, S.; Deng, L.; Khakh, K.; Chang, E.; Ho, H.; Shriver, S.; Young, C.; Lin, S.; Johnson, J.P., Jr.; et al. Structural basis of Nav1.7 inhibition by an isoform-selective small-molecule antagonist. *Science* **2015**, *350*, aac5464. [CrossRef] [PubMed]
87. Calandre, E.P.; Rico-Villademoros, F.; Slim, M. Alpha(2)delta ligands, gabapentin, pregabalin and mirogabalin: A review of their clinical pharmacology and therapeutic use. *Expert Rev. Neurother.* **2016**, *16*, 1263–1277. [CrossRef]
88. Wu, C.L.; Fu, P.; Cho, H.Y.; Chuang, T.H.; Wu, S.N. Evidence for Dual Activation of I(K(M)) and I(K(Ca)) Caused by QO-58 (5-(2,6-Dichloro-5-fluoropyridin-3-yl)-3-phenyl-2-(trifluoromethyl)-1H-pyrazolol [1,5-a]pyrimidin-7-one). *Int. J. Mol. Sci.* **2022**, *23*, 7042. [CrossRef]
89. Simasko, S.M. A background sodium conductance is necessary for spontaneous depolarizations in rat pituitary cell line GH3. *Am. J. Physiol.* **1994**, *266*, C709–C719. [CrossRef]
90. Sankaranarayanan, S.; Simasko, S.M. A role for a background sodium current in spontaneous action potentials and secretion from rat lactotrophs. *Am. J. Physiol.* **1996**, *271*, C1927–C1934. [CrossRef]
91. Navarro, M.A.; Salari, A.; Lin, J.L.; Cowan, L.M.; Penington, N.J.; Milescu, M.; Milescu, L.S. Sodium channels implement a molecular leaky integrator that detects action potentials and regulates neuronal firing. *Elife* **2020**, *9*, e54940. [CrossRef]
92. Guérineau, N.C.; Monteil, A.; Lory, P. Sodium background currents in endocrine/neuroendocrine cells: Towards unraveling channel identity and contribution in hormone secretion. *Front. Neuroendocrinol.* **2021**, *63*, 100947. [CrossRef]
93. Martiszus, B.J.; Tsintsadze, T.; Chang, W.; Smith, S.M. Enhanced excitability of cortical neurons in low-divalent solutions is primarily mediated by altered voltage-dependence of voltage-gated sodium channels. *Elife* **2021**, *10*, e67914. [CrossRef]
94. Wengert, E.R.; Patel, M.K. The Role of the Persistent Sodium Current in Epilepsy. *Epilepsy Curr.* **2021**, *21*, 40–47. [CrossRef]
95. Nakamura, M.; Jang, I.S. Contribution of tetrodotoxin-resistant persistent Na(+) currents to the excitability of C-type dural afferent neurons in rats. *J. Headache. Pain* **2022**, *23*, 73. [CrossRef]
96. Wu, S.N.; So, E.C.; Liao, Y.K.; Huang, Y.M. Reversal by ranolazine of doxorubicin-induced prolongation in the inactivation of late sodium current in rat dorsal root ganglion neurons. *Pain Med.* **2015**, *16*, 1032–1034. [CrossRef]
97. Gorman, K.M.; Peters, C.H.; Lynch, B.; Jones, L.; Bassett, D.S.; King, M.D.; Ruben, P.C.; Rosch, R.E. Persistent sodium currents in SCN1A developmental and degenerative epileptic dyskinetic encephalopathy. *Brain Commun.* **2021**, *3*, fcab235. [CrossRef]
98. Poulin, H.; Chahine, M. R1617Q epilepsy mutation slows Na(V) 1.6 sodium channel inactivation and increases the persistent current and neuronal firing. *J. Physiol.* **2021**, *599*, 1651–1664. [CrossRef]
99. Chao, E.C.; Henry, R.R. SGLT2 inhibition–a novel strategy for diabetes treatment. *Nat. Rev. Drug. Discov.* **2010**, *9*, 551–559. [CrossRef]
100. Sha, S.; Devineni, D.; Ghosh, A.; Polidori, D.; Chien, S.; Wexler, D.; Shalayda, K.; Demarest, K.; Rothenberg, P. Canagliflozin, a novel inhibitor of sodium glucose co-transporter 2, dose dependently reduces calculated renal threshold for glucose excretion and increases urinary glucose excretion in healthy subjects. *Diabetes Obes. Metab.* **2011**, *13*, 669–672. [CrossRef]
101. Brown, E.; Heerspink, H.J.L.; Cuthbertson, D.J.; Wilding, J.P.H. SGLT2 inhibitors and GLP-1 receptor agonists: Established and emerging indications. *Lancet* **2021**, *398*, 262–276. [CrossRef]
102. Philippaert, K.; Kalyaanamoorthy, S.; Fatehi, M.; Long, W.; Soni, S.; Byrne, N.J.; Barr, A.; Singh, J.; Wong, J.; Palechuk, T.; et al. Cardiac Late Sodium Channel Current Is a Molecular Target for the Sodium/Glucose Cotransporter 2 Inhibitor Empagliflozin. *Circulation* **2021**, *143*, 2188–2204. [CrossRef] [PubMed]
103. Catterall, W.A. From ionic currents to molecular mechanisms: The structure and function of voltage-gated sodium channels. *Neuron* **2000**, *26*, 13–25. [CrossRef]
104. Fletcher, P.A.; Sherman, A.; Stojilkovic, S.S. Common and diverse elements of ion channels and receptors underlying electrical activity in endocrine pituitary cells. *Mol. Cell Endocrinol.* **2018**, *463*, 23–36. [CrossRef]